ELSEVIER

Electrochemistry Communications 3 (2001) 20–23

electrochemistry communications

www.elsevier.nl/locate/elecom

New findings: structural changes in $LiAl_xMn_{2-x}O_4$

Yun Sung Lee [a], Hwack joo Lee [b], Masaki Yoshio [a,*]

[a] *Department of Applied Chemistry, Faculty of Science and Engineering, Saga University, 1 Honjo, Saga 840-8502, Japan*
[b] *Materials Evaluation Center, Korea Research Institute of Standards and Science, Yusung, Daejon 305-600, South Korea*

Received 9 October 2000; received in revised form 6 November 2000; accepted 6 November 2000

Abstract

$LiAl_{0.1}Mn_{1.9}O_4$ was synthesized using LiOH, $Al(NO_3)_3$ and two different Mn sources (γ-MnOOH and Mn_3O_4). The X-ray diffraction (XRD) analyses of the prepared materials revealed identical crystalline phases (cubic, Fd $\bar{3}$ m). The two $LiAl_{0.1}Mn_{1.9}O_4$ materials presented very good cycling performance in the 4 V region, but the $LiAl_{0.1}Mn_{1.9}O_4$ prepared using Mn_3O_4 showed a severe capacity fading in the 3 V region. It showed a mixed cubic and tetragonal phase which was detected from the XRD spectrum of the material discharged down to 2.2 V after 50 cycles. Meanwhile, it was observed that $LiAl_{0.1}Mn_{1.9}O_4$ synthesized using γ-MnOOH has only a tetragonal phase after the electrochemical test under the same conditions and had a higher capacity retention rate in the 3 V region. We now report the extraordinary electrochemical performances from the two $LiAl_{0.1}Mn_{1.9}O_4$ materials prepared using different manganese sources.

Keywords: Al-doped spinel; Manganese source; Structural change; Lithium battery

1. Introduction

The battery industries have aimed to supply safe power sources with high energy density and good cycle performance. Lithium secondary batteries are the most promising candidate among the many possibilities to satisfy this demand. Many researchers [1,2] have focused on the development of new cathode materials for lithium secondary batteries to realize the production of a high energy density battery.

The $LiMn_2O_4$ spinel has been widely investigated because of its low cost, environmental merit, and easy preparation method over the other cathode materials [3]. However, $LiMn_2O_4$ still shows significant capacity fading at high temperatures and poor cycleability when cycled in the 3 or $(3+4)$ voltage range. In the 3 V region, lithium inserts into the octahedral vacancy (16c site) of the spinel ($Li_xMn_2O_4$) structures $(1 < x \leqslant 2)$. This intercalation process brings about a Jahn–Teller distortion which induces an increase in the c/a ratio of the spinel unit cell of about 16%. The distorted spinel structure results in the capacity fading in this voltage range [4]. The origin of the poor cycleability of the $LiMn_2O_4$ spinel in the 4 V region has been suggested as follows: (1) slow dissolution of the $LiMn_2O_4$ electrode in the electrolyte by a disproportionation reaction ($2Mn^{3+} \rightarrow Mn^{4+} + Mn^{2+}$) [5], (2) unstable two-phase region in high voltage region [6], (3) electrolyte decomposition at high potentials [7], and (4) Jahn–Teller distortion in the deeply discharged state [8].

Recently, we synthesized Al-doped spinels ($LiAl_x Mn_{2-x}O_4$, $x = 0.03$–0.12) using various Al sources and two Mn sources to improve the cycle performance of the $LiMn_2O_4$ spinel. These materials showed excellent cycle performance as well as a high initial discharge capacity [9]. However, we found that $LiAl_xMn_{2-x}O_4$ materials prepared using different Mn starting materials showed different electrochemical properties in the 3 V region. Furthermore, they exhibited a unique structural change in the discharged state (~2.2 V).

In this paper, we report new results on the structural change and electrochemical behavior of Al-doped

* Corresponding author. Tel.: +81-952-28-8673; fax: +81-952-28-8591.
E-mail address: yoshio@ccs.ce.saga-u.ac.jp (M. Yoshio).

1388-2481/01/$ - see front matter
PII: S1388-2481(00)00140-5

spinels which were prepared using different Mn starting materials.

2. Experimental

The $LiAl_{0.1}Mn_{1.9}O_4$ materials were synthesized using LiOH, $Al(NO_3)_3$ and two different manganese sources. The Mn sources were Mn_3O_4 and γ-MnOOH, which were synthesized by Tosoh (Japan). The mixture of LiOH, $Al(NO_3)_3$ and Mn_3O_4 (or γ-MnOOH) was pre-calcined at 470°C and 530°C for 5 h in O_2 or air, respectively, and then post-calcined at 800°C for 24 h by the melt–impregnation method [10].

The powder X-ray diffraction (XRD, Rint 1000, Rigaku) using Cuk_α radiation was employed to identify the crystalline phase of the synthesized materials. Li, Al, and Mn contents in the resulting materials were analyzed using an atomic absorption spectrometer (AAS, Shimadzu, AA-6200). Transmission electron microscopy (TEM) specimens were prepared by mechanically punching the sample in the form of discs with a 3 mm diameter. The discs were then mechanically polished to a thickness of about 70 μm. The perforation of the specimen was carried out using a precision Ar ion miller (Model 691, Gantan, USA) with an acceleration voltage of 3 kV. The incident angle of the Ar ion on a specimen was 5° for the uniform thinning which produced no damage to the specimen. These samples were examined with a side-entry-type HRTEM (H-9000NAR) working at 300 kV with a point resolution of 0.18 nm. The electrochemical characterizations were performed using CR2032 coin-type cells and handmade screw cells for the structural change of the cathode materials after 50 cycles. The cathode was fabricated with 20 mg (or 25 mg for the screw cell) of accurately weighed active material and 13 mg (or 18 mg) of conductive binder (10 mg of Teflonized acetylene black (TAB) and 5 mg graphite). It was pressed on a 250 mm^2 stainless steel mesh used as the current collector under a pressure of 300 kg/cm^2 and dried at 200°C for 5 h in an oven. The test cell was made of a cathode and a lithium metal anode (Cyprus Foote Mineral) separated by a porous polypropylene film (Celgard 3401). The electrolyte was a mixture of 1 M $LiPF_6$–ethylene carbonate (EC)/dimethyl carbonate (DMC) (1:2 by volume). The charge and discharge current densities were 0.4 mA/cm^2 with a cut-off voltage of 2.0–4.3 V (or 2.2–3.6 V for the 3 V test).

3. Results and discussion

Table 1 shows that the powders are the same materials which have the typical physicochemical properties of $LiAl_{0.1}Mn_{1.9}O_4$. They also showed almost the same XRD pattern (Fd $\overline{3}$ m) except having different intensity ratios for the (3 1 1)/(4 0 0) peaks as reported in our previous study [9].

Fig. 1 shows the cycle characterization of the $LiAl_{0.1}Mn_{1.9}O_4$ materials prepared using two different manganese sources in the 3 and 4 V regions. The $LiAl_{0.1}Mn_{1.9}O_4$ materials synthesized using Mn_3O_4 and γ-MnOOH were designated as samples A and B, respectively. Both samples show very good battery performance in the 4 V region with the cycle retention rates of about 96 and 90% for samples A and B, respectively, after 50 cycles. However, the samples presented very different cycle behaviors in the 3 V region. After the 50th cycle, sample B shows a fairly high discharge capacity greater than 98.31 mAh/g in the 3 V test, while sample A (40.53 mAh/g) exhibits a discharge capacity lower than that of sample B. It is very interesting to note the decrease in the reversibility of sample A with cycling in the 3 V region even if the two materials have almost the same composition. Moreover, the capacity difference between samples A and B after the 50th cycle in the $(3 + 4)$ V region reached 97 mAh/g.

In order to interpret this extraordinary behavior observed from the $LiAl_{0.1}Mn_{1.9}O_4$ materials, ex-situ XRD measurements were taken for samples A and B in the discharged state after 50 cycles. Each cell was left in a dry room for 2 days to reach equilibrium after the cycling and the electrode was washed with DMC solution to remove the $LiPF_6$ salt.

The XRD patterns for the prepared materials and electrodes discharged to 2.2 V after 50 cycles of $LiMn_2O_4$, sample A, and sample B are shown in Fig. 2, respectively. The two $LiAl_{0.1}Mn_{1.9}O_4$ materials showed the same XRD pattern as shown in Figs. 2(a) and (b). On the other hand, Figs. 2(d) and (e) showed entirely different XRD patterns in the discharged state after 50 cycles. Sample A still keeps both cubic and tetragonal phases together, whereas sample B shows an almost perfect $Li_2Mn_2O_4$ (tetragonal) structure after 50 cycles.

Many research groups have already reported that the Jahn–Teller distortion is the main reason for including a capacity loss in the 3 V region of the $LiMn_2O_4$ system [4,11]. When $LiMn_2O_4$ discharged perfectly in the 3 V

Table 1
Properties and chemical analysis data of $LiAl_{0.1}Mn_{1.9}O_4$

$LiAl_{0.1}Mn_{1.9}O_4$ ($LiOH + AlNO_3 + Mn$)	Li (wt%)	Al (wt%)	Mn (wt%)	2Li/M (M = Al + Mn)	Lattice parameter (Å)	Surface area (m^2/g)
Mn_3O_4	3.91	1.32	58.79	1.008	8.2273	2.574
γ-MnOOH	3.93	1.34	59.47	1.007	8.2231	2.681

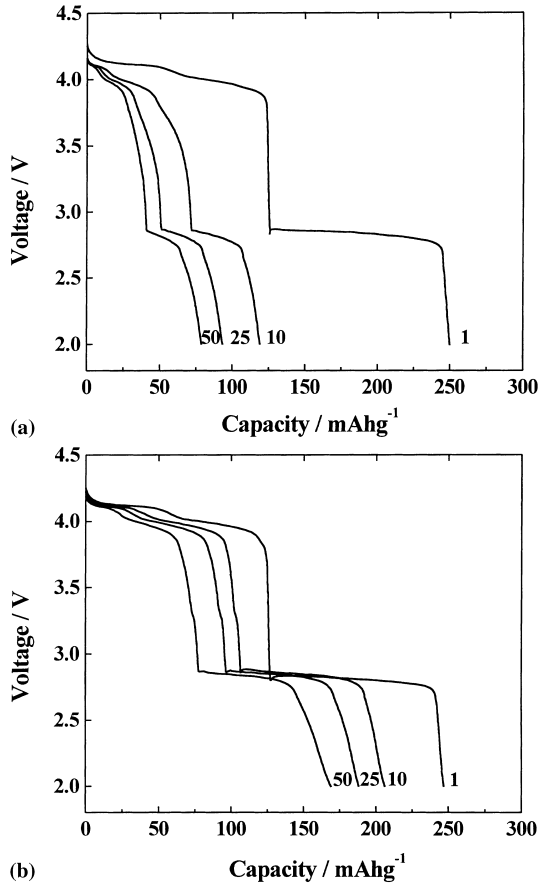

Fig. 1. Discharge curves with the number of cycles for the Li/1 M $LiPF_6$–EC/DMC/$LiAl_{0.1}Mn_{1.9}O_4$ cells. (a) $LiAl_{0.1}Mn_{1.9}O_4$ using Mn_3O_4; (b) $LiAl_{0.1}Mn_{1.9}O_4$ using γ-MnOOH. Cycling was carried out at a constant harge–discharge current density of 0.4 mA/cm^2 between 2.0 and 4.3 V.

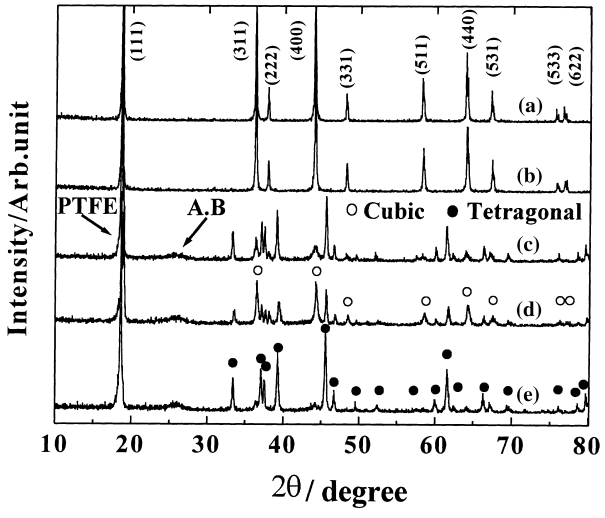

Fig. 2. XRD patterns in the 3 V region. (a) $LiAl_{0.1}Mn_{1.9}O_4$ using Mn_3O_4; (b) $LiAl_{0.1}Mn_{1.9}O_4$ using γ-MnOOH; (c) $LiMn_2O_4$ after 50 cycles; (d) $LiAl_{0.1}Mn_{1.9}O_4$ using Mn_3O_4 after 50 cycles; (e) $LiAl_{0.1}Mn_{1.9}O_4$ using γ-MnOOH after 50 cycles.

region, it causes a phase transformation of the material from cubic to tetragonal $Li_2Mn_2O_4$ by insertion of lithium deintercalated from the Li anode, which is indexed into a face-centered tetragonal unit ($14_1/amd$). However, an imperfect charge–discharge process, which results from Jahn–Teller distortion or other effects, brings about the coexistence of the cubic and tetragonal phases, which encouraged an incomplete lithium insertion/extraction reaction (Fig. 2(c)) [12].

Recently, Sun et al. [13] synthesized a new sulfur-doped spinel ($LiAl_{0.24}Mn_{1.76}O_{3.98}S_{0.02}$) material and observed an excellent cycle performance from this material even in the 3 and $(3 + 4)$ V regions. They reported that this is because the material retains its original cubic structure even in the 3 V region. However, in our research, it was observed that sample A exhibits severe capacity fading in the 3 V region although the cubic phase remained after the cycling. However, sample B shows a fairly good cycle performance in all the potential ranges (2.0–4.3 V) although its structure completely changed into the tetragonal phase. It is worth noting that this is a new observation different from the previous reports.

TEM measurements were employed to clarify the different structural changes in the $LiAl_{0.1}Mn_{1.9}O_4$. The same electrodes studied in ex-situ XRD analysis were used for these measurements. Fig. 3 shows the selected area electron diffraction (SAD) patterns of the lattice image of the $LiAl_{0.1}Mn_{1.9}O_4$ materials. Fig. 3(a) and (b) present the SAD patterns of samples A and B, respectively. Because the cubic and tetragonal structures have almost the same SAD pattern except for the appearance of the (0 2 2) reflection in the [1 0 0] zone, the distinct difference between the two structures can be easily recognized by detecting the existence of the (0 2 2) reflection in the [1 0 0] zone axis [8]. However, it seems from Fig. 3(a) that sample A has only a cubic spinel structure although a mixture of the cubic and tetragonal phases was detected from the ex-situ XRD analysis of the same sample. Based on the assumption that these two structures coexist, the overlapped pattern of the two structures might show the same SAD pattern as the pure cubic structure. Therefore, Fig. 3(a) is not the SAD pattern of the pure cubic structure, but is an overlapped pattern of the cubic and tetragonal structures. Meanwhile, Fig. 3(b) shows the SAD pattern of the tetragonal phase, indicating that sample B has a tetragonal structure. The above observation obviously indicates that, when the electrodes were discharged down to 2.2 V, sample A has a mixed structure of the cubic and tetragonal phases, whereas sample B has only the tetragonal structure.

It may be concluded from these results that the $LiAl_{0.1}Mn_{1.9}O_4$ materials, which were synthesized using different manganese starting materials, can show different structural changes in the lower voltage region although they have the same composition. Further work is now in progress on the reaction mechanism and main

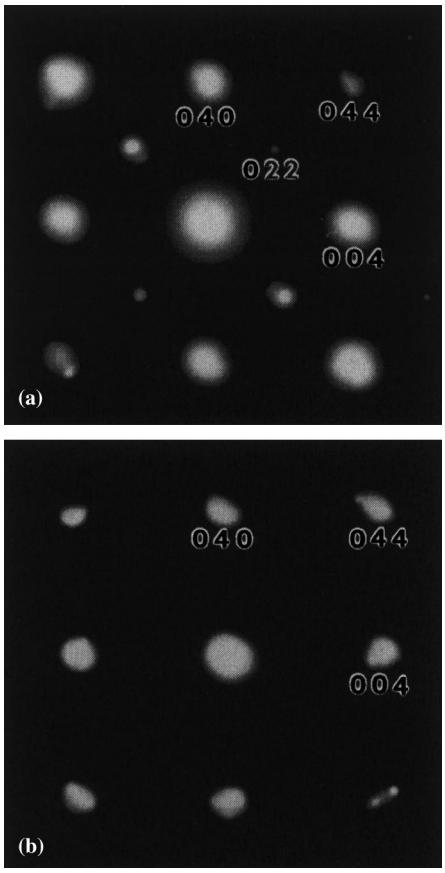

Fig. 3. SAD patterns ([1 0 0] zone axis) of $LiAl_{0.1}Mn_{1.9}O_4$ (a) $LiAl_{0.1}Mn_{1.9}O_4$ using Mn_3O_4, and (b) $LiAl_{0.1}Mn_{1.9}O_4$ using γ-MnOOH.

reason for inducing the different electrochemical performance of $LiAl_{0.1}Mn_{1.9}O_4$ in the 3 and $(3+4)$ V regions.

4. Conclusion

The $LiAl_{0.1}Mn_{1.9}O_4$ materials were prepared by the melt–impregnation method using LiOH, $Al(NO_3)_3$ and two different manganese sources. The $LiAl_{0.1}Mn_{1.9}O_4$ synthesized using Mn_3O_4 showed a severe capacity fading in the 3 V region although it retains the cubic spinel phase when discharged down to 2.2 V. However, the $LiAl_{0.1}Mn_{1.9}O_4$ synthesized using γ-MnOOH exhibited a good cycle performance in all the 3 and $(3+4)$ V regions although its structure becomes tetragonal under the same test conditions. These results were confirmed by the ex situ XRD and TEM measurements. It was concluded that this might be an important clue to reveal the different electrochemical properties of the $LiAl_{0.1}Mn_{1.9}O_4$ materials which were prepared using different Mn sources.

References

[1] J.N. Reimers, E.W. Fuller, E. Rossen, J.R. Dahn, J. Electrochem. Soc. 140 (1993) 3396.
[2] T. Ohzuku, A. Ueda, M. Nagayama, J. Electrochem. Soc. 140 (1993) 1862.
[3] J.M. Tarascon, W.R. Mckinnon, F. Coowar, T.N. Bowmer, G. Amatucci, D. Guyomard, J. Electrochem. Soc. 141 (1994) 1421.
[4] J. Barker, R. Koksbang, M.Y. Saidi, Solid State Ionics 82 (1995) 143.
[5] D.H. Jang, Y.J. Shin, S.M. Oh, J. Electrochem. Soc. 143 (1996) 2204.
[6] Y. Xia, Y. Zhou, M. Yoshio, J. Electrochem. Soc. 144 (1997) 2593.
[7] D. Guyomard, J.M. Tarascon, J. Electrochem. Soc. 139 (1992) 937.
[8] M.M. Thackeray, Y. Shao-Horn, A.J. Kahaian, K.D. Kepler, E. Skinner, J.T. Vaughey, S.A. Hackney, Electrochem. Solid-State Lett. 1 (1) (1998) 7.
[9] Y.-S. Lee, N. Kumada, M. Yoshio, J. Power Sources, 2000 (accepted).
[10] Y. Xia, H. Takeshige, H. Noguchi, M. Yoshio, J. Power Sources 56 (1995) 61.
[11] M.M. Thackeray, A. de Kock, M.H. Rossouw, D. Liles, R. Bittihn, D. Hodge, J. Electrochem. Soc. 139 (1999) 363.
[12] J.B. Goodenough, M.M. Thackeray, W.I.F. David, P.G. Bruce, Rev. Chim. Miner. 21 (1984) 435.
[13] Y.-K. Sun, Y.-S. Jeon, H.J. Lee, Electrochem. Solid-State Lett. 3 (1) (2000) 7.